Chemoselective, oxidation-induced macrocyclization of tyrosine-containing peptides

E. Dalles Keyes,[†] Marcus. C. Mifflin,[†] Maxwell J. Austin,[†] Brighton J. Alvey,[†] Lotfa H. Lovely,[†] Andriea Smith,[†] Bethany A. Buck-Koehntop,[†] and Andrew G. Roberts[†,*]

[†]Department of Chemistry, University of Utah, 315 South 1400 East, Salt Lake City, Utah 84112, United States

KEYWORDS. tyrosine, phenols, cyclic peptides, triazolinediones, macrocyclization, peptide cyclization

ABSTRACT: Inspired by Nature's wide range of oxidation-induced modifications to install cross-links and cycles at tyrosine (Tyr) and other phenol-containing residue side chains, we report a Tyr-selective strategy for the preparation of Tyr-linked cyclic peptides. This approach leverages N4-substituted 1,2,4-triazoline-3,5-diones (TADs) as azo electrophiles that react chemoselectively with the phenolic side chain of Tyr residues to form stable C–N1-linked cyclic peptides. In the developed method, a precursor 1,2,4-triazolidine-3,5-dione moiety, also known as a urazole, is readily constructed at any free amine revealed on a solid-supported peptide. Once prepared, the N4-substituted urazole peptide is selectively oxidized using mild, peptide-compatible conditions to generate an electrophilic N4-substituted TAD peptide intermediate that reacts selectively under aqueous conditions with internal and terminal Tyr residues to furnish Tyr-linked cyclic peptides. The approach demonstrates good tolerance of native residue side chains and enables access to cyclic peptides ranging from 3- to 11-residues in size (16- to 38-atom-containing cycles). The identity of the installed Tyr-linkage, a stable covalent C–N1 bond, was characterized using NMR spectroscopy. Finally, we applied the developed method to prepare biologically active Tyr-linked cyclic peptides bearing the integrin-binding RGDf epitope.

Introduction

Peptide natural products have long served as inspiration for developing new therapeutics to treat human diseases.[1] Therapeutic peptides commonly exhibit effective protein-target binding activity at low concentrations as a result of high selectivity and offer an inherent advantage of amino acid degradation products being minimally toxic.[2–4] However, the value of peptide therapeutics is often overshadowed by a marked susceptibility to proteolytic degradation and subsequent failure to reach a validated target in vivo. The modification of bioactive linear peptides by cyclization has been shown to be an effective strategy for addressing this problem.[5–10] In fact, the bioactivity and pharmacokinetic profiles of constrained cyclic peptides are often improved relative to their acyclic counterparts.[11]

Among Nature's wide range of peptide cyclization strategies, the oxidative coupling of aromatic amino acid sidechains has drawn considerable interest. Proteinogenic tyrosine (Tyr) residues are often involved in structure-altering oxidative cyclization events via the generation of tyrosyl radicals and related intermediates.[12,13] Such redox active intermediates are notably involved in the formation dityrosine and isodityrosine protein cross-links (**Figure 1A**). While these biaryl linkages are frequently identified as clinical markers of oxidative stress and aging, they have been shown to impart beneficial structural stability and elasticity to peptide and protein-based systems.[14–16] Similar transformations are commonly observed in natural product biosynthesis pathways, resulting in structurally constrained mono- and polycyclic peptides with promising and diverse biological activities.[17] Exemplary biaryl-linked cyclic peptides that derive from phenolic-residue oxidation include the angiotensin-converting enzyme inhibitor, K-13 **1** (C–O-linked), myxarylin **2** (C–N-linked), and C–C-linked antimicrobial peptides such as arylomycin A_2 **3** (**Figure 1A**).[18–23]

The desirable properties associated with cyclic peptides have motivated the development of creative synthetic methods to prepare cyclic peptides. Many of these strategies leverage the reactivity of free termini and residue side chain functionality, while others have introduced noncanonical residues to achieve site-selective cyclizations.[5,24,25] Nature forms stable covalent linkages by using oxidative manifolds to impart structural rigidity and stability to proteolytic degradation. However, replicating the linkages formed in Tyr- and hydroxyphenylglycine (Hpg)-containing cyclic peptides with

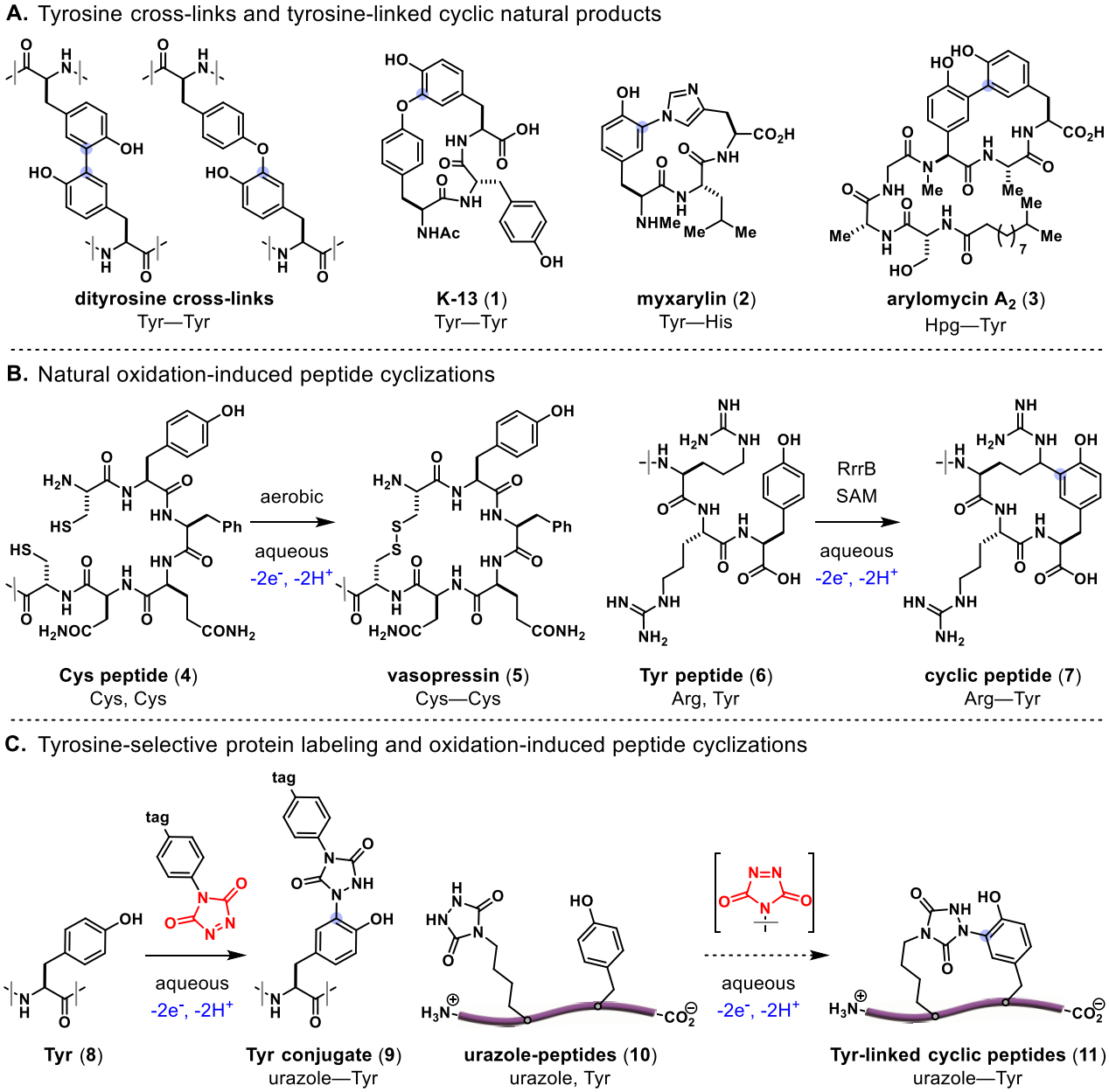

Figure 1. A. Tyrosine cross-links and cross-linked natural products: dityrosine, K-13, myxarylin, and arylomycin A2, **B.** Natural oxidative peptide cyclization: generation of vasopressin (**5**) under aerobic conditions through disulfide formation. Enzyme-mediated oxidation of Arg by RrrB SAM in a Tyr containing peptide gives a unique Arg–Tyr cross-link and cyclic peptide (**6**→**7**). C. Tyr-selective protein labeling: TAD-based reagents react chemoselectively with Tyr in protein labeling experiments (**8**→**9**). Proposed peptide cyclization strategy wherein Tyr selectively reacts with an intramolecular TAD to generate a Tyr-linked cyclic peptide (**10**→**11**).

chemoselective control presents significant challenges. In view of their desirable properties, the need for developing efficient synthetic methodologies to access cyclic peptides is clear. Synthetic access to these types of linkages is often enabled through multistep approaches which use transition metal-catalyzed couplings (*e.g.*, Suzuki couplings) or nucleophilic aromatic substitution as key reactions at residues with prefunctionalized phenolic side chains.[26–28] Emerging residue-selective protein modification and labeling methods have shown great potential for the controlled functionalization of peptides. For example, Baran and coworkers recently reported a Cu-mediated oxidative phenol coupling to achieve scalable access to the biaryl-linked 14-atom macrocyclic core that is common to the arylomycins.[29] Although transition metal-mediated strategies have enabled synthetic access to bioactive Tyr-linked cyclic peptides, few of these methods leverage the inherent nucleophilicity of phenolic side chains.[31-41] Recently, synthetic and chemoenzymatic strategies for preparing related variations of this

common macrocyclic core on scales suitable for manufacture were described by Gosselin and coworkers.[41] However, the generality has not been demonstrated for peptides containing diverse amino acid residue functionality or extended beyond three residue precursors to access to larger biaryl-linked macrocycles. The underdeveloped reactivity of its phenolic side chain presents a novel platform to develop Tyr-selective peptide cyclization methods. Considering the need for such strategies, we drew inspiration from the simplicity of other oxidation-induced cyclizations that occur spontaneously under aerobic conditions for peptides containing multiple cysteine (Cys) residues, such as the facile conversion of **4** into vasopressin **5**, and enzymatically, such as the remarkable conversion of **6** into C–C bond linked cyclic peptide **7**.[42–44] Given the prevalence of Tyr-linked cyclic peptide natural products, we set out to develop a method for the oxidatively-induced cyclization of Tyr-containing peptides.

In 2010, Barbas and coworkers developed the use of N4-substituted 1,2,4-triazoline-3,5-diones (TADs) reagents for Tyr-selective protein bioconjugation (**Figure 1C**).[45] These aqueous-compatible reactions are described as 'click-like' by virtue of their favorable reaction rates and residue-selectivity. Accordingly, many TAD reagents have been prepared for protein bioconjugation studies, discriminating changes in protein structure,[46] and recent electrochemical oxidation methods have been developed to enable the *in situ* generation of N4-substituted TAD reagents from their corresponding N4-substituted urazole precursors.[47–51] The procedural ease of these developments encouraged us to examine scenarios where *in situ* generated N4-substituted TAD peptides could react with sequence-embedded Tyr residues to produce Tyr-linked cyclic peptides (**Figure 1C**). The method design was predicated on several objectives. We sought to (1) provide predictable and modular access to Tyr-linked cyclic peptides, using (2) peptide-compatible oxidation conditions that tolerate native residue functionalities, while (3) being procedurally simple to perform. In this approach, we show N4-substituted urazoles are readily built using *N*-terminal or embedded amines of Tyr-containing peptides. The urazole moiety can be chemoselectively oxidized *in situ* to generate a N4-substituted TAD peptide that undergoes spontaneous cyclization with an embedded Tyr residue under aqueous conditions.

Synthesis of urazole-containing peptides.

We began with the development of a general procedure to prepare urazole-containing peptides **14** (**Figure 2**). Despite the utility of urazole-containing peptides in labeling and protein bioconjugation applications, strategies for their assembly are underdeveloped.[52] Our initial approach evaluated a method reported by Börner and coworkers wherein a N4-substituted urazole can be built from an *N*-terminal amine of a solid supported peptide.[53]

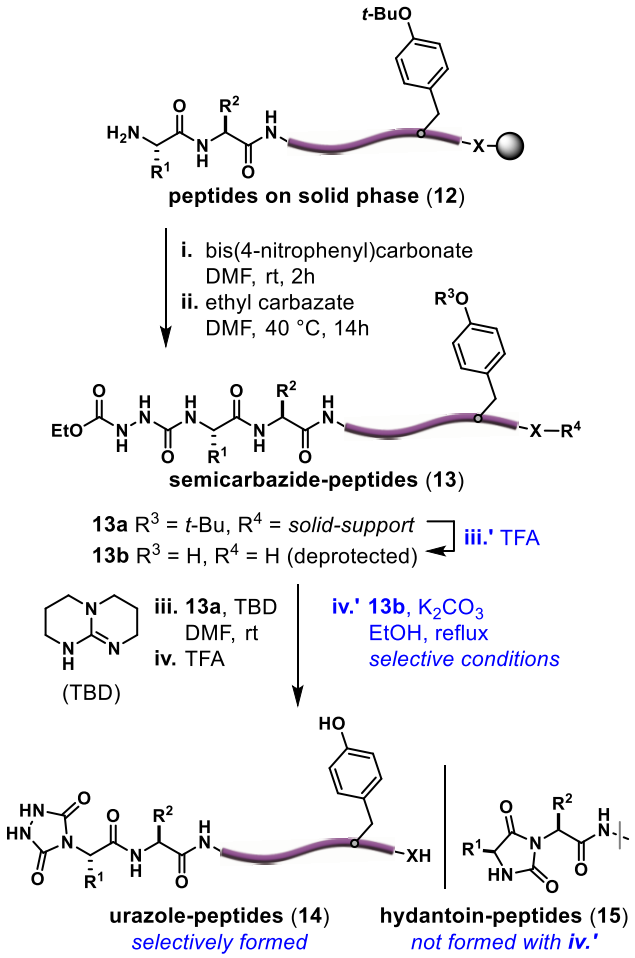

Figure 2. Strategies for preparing urazole-peptides (**14**): Peptides on solid phase (**12**) react in two steps to form semicarbazide-peptides (**13**). Upon cleavage from resin, semicarbazide-peptides (**13b**) react with K_2CO_3 in refluxing ethanol to selectively provide urazole-peptides (**14**) and the conditions avoid hydantoin-peptide (**15**) formation in sequences bearing acyclic residues at position-2.

Here, the *N*-terminal amine at position-1 (**12**) reacts with bis(4-nitrophenyl)carbonate to provide a carbamate *en route* to a semicarbazide intermediate (**13a**) (see the *Supplementary Information*). Treatment of the semicarbazide intermediate (**13a**) on solid support with 1,5,7-triazabicyclo[4.4.0]dec-5-ene (TBD) promotes cyclization to form the desired urazole-peptide (**14**) following acid-promoted cleavage and global deprotection. Unfortunately, we found this method limited to sequences bearing proline (Pro) or a pseudoproline residue at position 2, as deviations from this led to undesirable hydantoin-peptide (**15**) formation during the cyclization step.

We were unable to find suitable conditions to prepare urazole-containing peptides (**14**) on solid support, prompting the development of an alternative and selective strategy. First, we optimized conditions to access

deprotected semicarbazide-peptides (**13b**) following steps i., ii, and iii.' (**Figure 2**). We found the cyclization of semicarbazide-peptides **13b** using alkaline conditions (step iv.' K_2CO_3, EtOH, reflux) in solution to provide general access to urazole-peptides (**14**) in good overall yields while avoiding hydantoin-peptide (**15**) formation.[54] Over 20 urazole-peptides (**14**) have been prepared using this strategy, including those that bear acyclic residues at position-2 (*e.g.*, Xaa_2 = Ala_2) (see the *Supplementary Information*).

Chemoselective peptide cyclization at tyrosine.

With urazole-containing peptides (**14**) in hand, we next identified mild conditions to access Tyr-linked cyclic peptides (**16**). We envisioned a one-pot strategy wherein oxidation of urazole peptides (**14**) would generate reactive TAD peptides (***int*-16**) *in situ* that could undergo spontaneous cyclization at an embedded Tyr residue to access Tyr-linked cyclic peptides (**16**) (**Figure 3**). This strategy presented several compatibility challenges, as the urazole oxidation conditions must be selective and tolerant of native amino acid residue side chain functionalities. At the onset of our investigations, biocompatible electrochemical urazole oxidation methods were unknown.[48,55] Moreover, there was no information regarding the spontaneity of cyclization events provided TAD peptides (***int*-16**) could be efficiently formed. These challenges necessitated the identification of conditions to, first, generate TAD peptides (***int*-16**) selectively and second, induce cyclization with an embedded Tyr residue to provide cyclic peptides (**16**). Using **14d** as a model sequence, preliminary studies evaluated inorganic and organic nitrite reagents as potentially suitable oxidants. Sodium nitrite ($NaNO_2$) is known to efficiently promote the oxidation of urazoles to TADs and has demonstrated tolerance of amino acid residue functionality.[56–58] Indeed, when an acidic solution of **14d** (0.19 M, 1 equiv) in acetonitrile was treated with $NaNO_2$ (1.0 equiv), the presumed TAD intermediate (see ***int*-16**) was readily generated *in situ* as qualitatively observed by the immediate change from colorless to a carmine red color that has been characteristically attributed to the extended azo chromophore of TADs (UV λ_{max} = 532 nm).[59] Based on conditions developed for protein bioconjugation with N4-aryl TAD derivatives, we attempted to induce cyclization by diluting the presumed TAD-containing solution with a phosphate buffered acetonitrile-water solution (1:1 CH_3CN/100 mM phosphate buffer (PB), pH = 7.0).[47] Unfortunately, mass spectrometry analysis indicated that TAD intermediate hydrolysis and Tyr residue nitration occurred alongside a significant amount of unreacted **14d**.[60] This result can be partly rationalized by the limited solubility of $NaNO_2$ in organic solvents, which, despite the observable TAD formation, could have suppressed the reaction efficiency. To address this issue, we evaluated the reactivity of *tert*-butyl nitrite, *t*-$BuNO_2$, due to its greater solubility in organic solvents. Following the oxidation of **14d** (1 equiv) with *t*-$BuNO_2$ (1.3 equiv) in acidic acetonitrile (1 vol% AcOH in CH_3CN), the formed TAD intermediate (***int*-16d**) was subsequently diluted with a phosphate buffered acetonitrile-water solution. Still, products of TAD hydrolysis and oxidation at the Tyr residue remained prevalent. The hydrolysis result is consistent with a recent study from Heise and coworkers that evaluated the rate of N4-alkyl TAD hydrolysis in mixed aqueous-organic solutions.[61] From this, we hypothesized that TAD hydrolysis pathways could be suppressed by decreasing the dilutant water content. Accordingly, a solution of *in situ* formed TAD intermediate (***int*-16d**) was diluted into a phosphate buffered acetonitrile-water solution (3:2 CH_3CN/100 mM PB, pH = 7.0) and analysis of the mixture indicated the formation of a new product as observed by analytical LC with UV-detection. The suspected cyclic peptide (**16d**) exhibited increased polarity relative to **14d** as observed by a shift in retention time. Mass spectrometric analysis of the collected peak revealed a monoisotopic mass of 545.2 Da, consistent with the anticipated $[M+H]^+$ ion for cyclic peptide **16d**. Encouraged by this result, these conditions were used to synthesize cyclic peptides **16a**–**16h** (**Figure 3**, using *condition A*). Nevertheless, we regularly observed incomplete consumption of **14**, as well as some undesirable byproducts that we presume to derive from oxidation at Tyr. Therefore, we continued to evaluate aqueous compatible oxidants for the improved *in situ* formation of TAD-containing peptides (***int-16***). Chlorinating reagents such as *t*-butyl hypochlorite and trichloroisocyanuric acid in DMF affected the oxidation, but promiscuous overoxidation resulted in low yields of isolated **16d** (**Figure S132**, see the *Supplementary Information*).[58,62] However, we discovered that oxidations using *N*-chlorosuccinimide (NCS) in DMF reduced the production of overoxidation products and provided **16d** in an improved 54% isolated yield. The comparatively improved yield for the model system supported the general use of NCS and all subsequent cyclizations were conducted using these conditions.[63]

Upon establishing conditions to selectively generate TAD-containing peptides (***int*-16**), we focused on solution pH optimization to improve the cyclization event (**Figure S133**, see the *Supplementary Information*). Seminal studies conducted by Barbas and coworkers demonstrated the pH sensitivity of the conjugation of N4-phenyl urazole (PTAD) and a model Tyr residue. This led us to evaluate cyclization efficiencies using phosphate-buffered acetonitrile-water conditions at pH = 7.0, 8.0, 9.0, and 10.0.[45] Ultimately, solution pH = 8.0 was found optimal for cyclization, affording **16d** in 64% isolated yield (**Figure 3**). This protocol (*condition B*: 1.1 equiv NCS and 1.1 equiv pyridine in DMF; dilute into 3:2 CH_3CN/100 mM PB at pH = 8.0) was applied to efficiently access 14 size- and sequence-diverse cyclic peptides in good yields

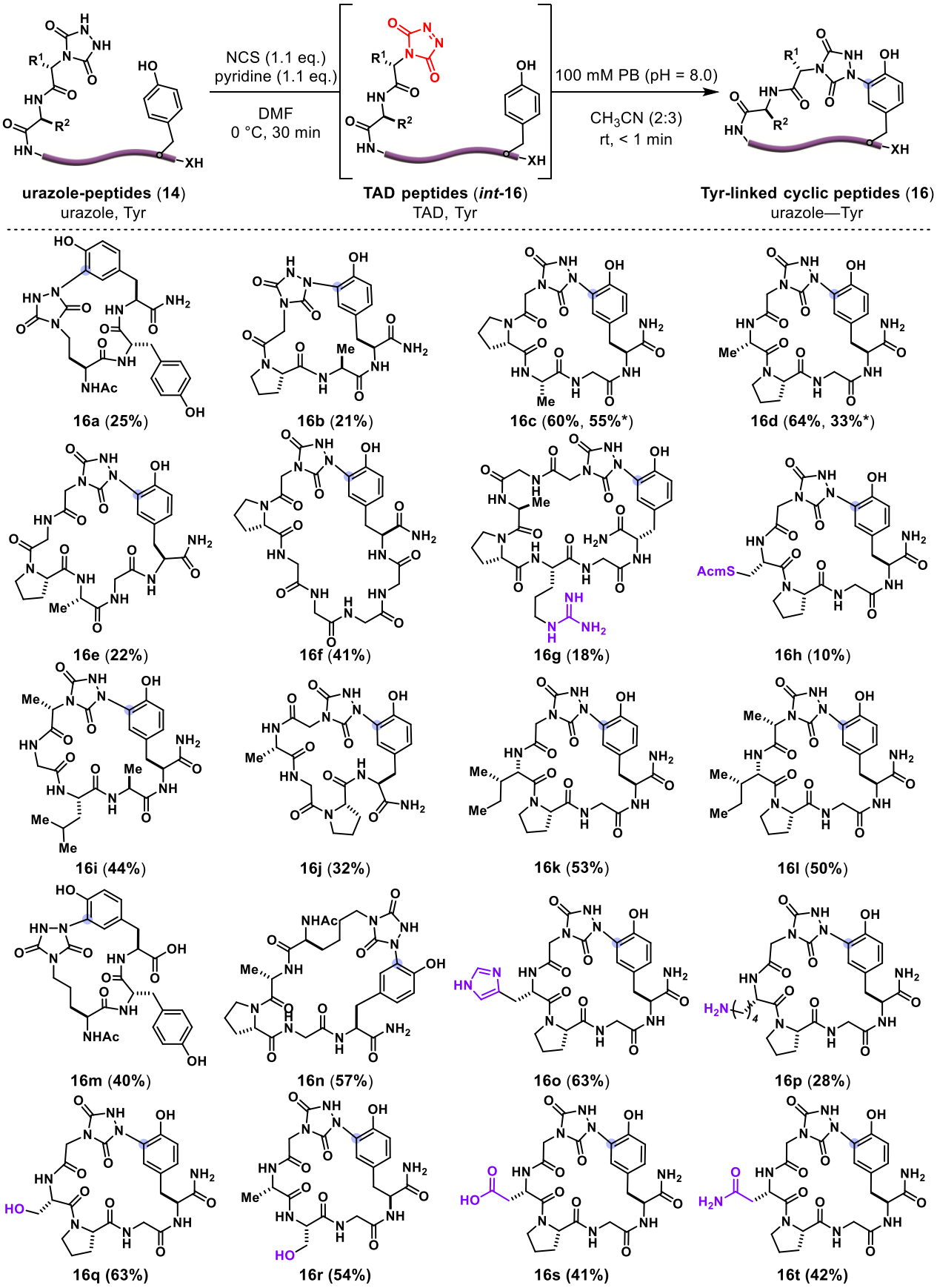

Figure 3. Tyr-linked cyclic peptides generated from *in situ* formed TAD-peptide intermediates.

(**Figure 3**). Notably, this general procedure exhibits high amino acid residue side chain tolerance, being compatible with native histidine (**16o**), lysine (**16p**), serine (**16q** and **16r**), aspartic acid (**16s**), asparagine (**16t**), and arginine (**16y** and **16z**, *vide infra*) residue side chain functionalities. Oxidation of substrates containing Cys or tryptophan (Trp) residues result in complex mixtures, likely the result of thiol (Cys) and indole (Trp) oxidation and their orthogonal nucleophilic reactivity toward-TADs.[64,65] However, the use of an acetamidomethyl (Acm) protection strategy together with oxidation condition *A* reduced side reactions for Cys residue-containing substrates, as demonstrated by access to cyclic peptide **16h**. Overall, we have developed a procedurally simple peptide cyclization method which provides facile access to a representative collection of Tyr-linked cyclic peptides (**16**) from native peptide sequences under aqueous conditions. We anticipate that the use of electrochemical oxidation methods for the *in situ* generation of TADs will expand the utility of this approach by enabling orthogonality to native, oxidation-prone residues. Such strategies are currently being explored in our laboratory.

Characterization of linear and cyclic peptides.

As previously described, the *in situ* generation of TAD-containing peptides (***int*-16**) is qualitatively observed by the characteristic solution color change to carmine (**Figure 4A**). The reactivity of these intermediates (***int*-16**), generated in the presence of Tyr residues, precludes their isolation by reverse-phase HPLC. While optimizing the oxidation and cyclization events using analytical methods that involve diluting reaction aliquots in water (*e.g.*, RP-HPLC analysis with UV-detection), only urazole-containing peptides (**14**), cyclic peptides (**16**), and minor byproducts were observed. Intriguingly, the carmine color of in situ generated solution of ***int*-16** dissipates within minutes of diluting with the phosphate buffered acetonitrile-water solution. This suggests TAD-peptides (***int*-16**) are rapidly cyclized to give cyclic peptides (**16**) under these conditions. Following purification, a comparison of the analytical HPLC chromatograms for acyclic (**14**) and cyclic peptides (**16**) shows that cyclization induces a general polarity change. This property is exemplified by the comparative chromatograms for urazole-containing peptide **14i** (t_R = 11.6 min) and cyclic peptide **16i** (t_R = 11.1 min) as shown in **Figure 4C**. Notably, this characteristic polarity change is conserved in 23 of the 26 examples presented in this work (Δt_R = 0.5 – 3.0 min., see the *Supplementary Information*).

To confirm the structural identity of the linkage in **16**, selected examples, **16d** and **16e**, were characterized by ^{1}H, ^{13}C, and 2-D nuclear magnetic resonance (NMR) spectroscopy experiments. In general, the comparative analysis of ^{1}H NMR spectra for acyclic (**14**) vs. cyclic (**16**) peptides rapidly reveals the structural change that

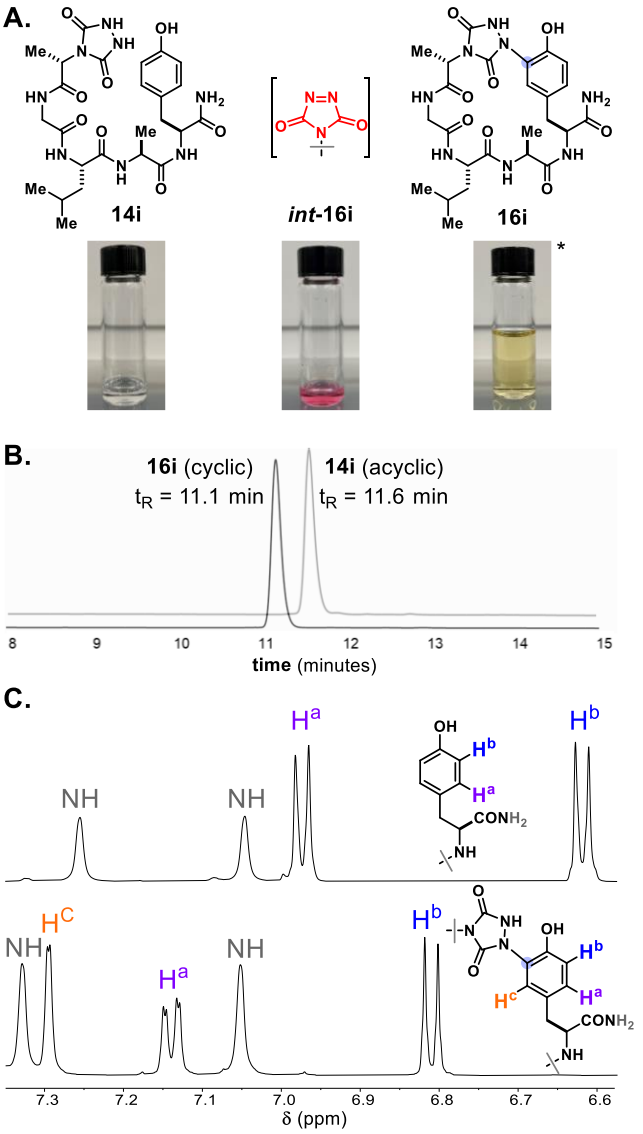

Figure 4. Characterization of **14i** and **16i**. **A.** Qualitative monitoring of reaction progress: oxidation of urazole-peptide **14i** (colorless) gives TAD-peptide **int-16i** (pink/carmine) which cyclizes to provide **16i** upon dilution with aqueous buffer, indicated by rapid dissipation of the pink color. **B.** Comparison of analytical RP-HPLC chromatograms for **14i** and **16i** demonstrates the polarity increase upon cyclization. **C.** Comparison of ^{1}H NMR spectra for **14i** and **16i** shows characteristic ABX splitting from the desymmetrization of Tyr. [a] crude reaction mixture containing **16i**.

occurs upon cyclization. This is demonstrated in a comparison of ^{1}H NMR spectra of **14i** and **16i**, wherein a diagnostic ABX signal is observed at 7.14 ppm (dd, J = 8.5, 2.2 Hz) in **16i** indicating the asymmetry of the trisubstituted Tyr residue (**Figure 4B**). Moreover, analysis of **16c** and **16d** by gHMBCAD and gHMQC 2-D NMR experiments support the Tyr-linked connectivity in cyclic peptides (**16**) (see the *Supplementary Information*).

Selectivity studies.

The breadth of tolerated residues and the cyclic peptide variability (3-7 residues, 16-26 atom-containing macrocycles) accessible using a TAD-based cyclization strategy is showcased by the 20 examples of Tyr-linked peptides (**16**) in **Figure 3**. We were interested in expanding the scope of this strategy with regards to macrocycle size, location of Tyr (*i.e.*, embedded *vs.* terminal), and site-selectivity when two Tyr residues are incorporated. Remarkably, 11-mer **14u** is readily converted into cyclic peptide **16u** in 21% isolated yield, despite the larger, 38-atom-containing ring size and presence of potentially reactive Ser, Arg, and His residue side chain functionality (**Figure 5A**). This example demonstrates the potential utility of our approach for generating cyclic peptides from longer sequences that bear diverse residue side chain functionalities.[66]

Due to the therapeutic potential of lariat peptides, which can exhibit improved cell permeability relative to acyclic and head-to-tail macrocyclic variants,[67] we evaluated the cyclization of **14v** to demonstrate access to lariat-type peptide **16v** that bears a Tyr residue at an embedded position (**Figure 5B**). Consistent with previous cases, **16v** was efficiently formed in 45% isolated yield, indicating this strategy can be used to access peptides with diverse structures, including lariat-type peptides.

Because peptides **16a** and **16m** were the only cyclic products produced from the oxidation of urazole-peptides **14a** and **14m**, we were interested in better understanding the product distributions that result from the cyclization of TAD peptides in sequences bearing multiple Tyr residues. Thus, we examined the cyclization of designed sequence **14w** which is flanked by Tyr residues at both the *N*- and *C*-termini. Surprisingly, evaluation of the crude reaction mixture by RP-HPLC revealed an approximate 4:1 distribution of cycles which, upon further analysis by 2D-NMR ^{1}H-^{13}C gHMQC and ^{1}H-^{13}C gHMBCAD experiments, were assigned to **16w** and **16x**, respectively (**Figure 5C**). These results support a preferential reaction of the TAD moiety with *N*-terminal Tyr residues, which may have utility for performing selective cyclizations. Together with previous cases, this result supports positioning the Tyr residue within a native peptide at least three residues away from the TAD moiety for successful cyclizations.

Biological activity.

We next set out to evaluate the utility of our approach for synthesizing cyclic peptides which exhibit biological activity. We prepared **16y** and **16z** as mimics of cilengitide, an anti-angiogenic cyclic pentapeptide bearing the RGDf epitope responsible for its antagonistic activity toward the integrins αvβ3 and αvβ5, as well as its low nanomolar binding affinity to α5β1 (**Figure 6A**).[68–74] We examined the activity of cycles **16y** and **16z** relative to

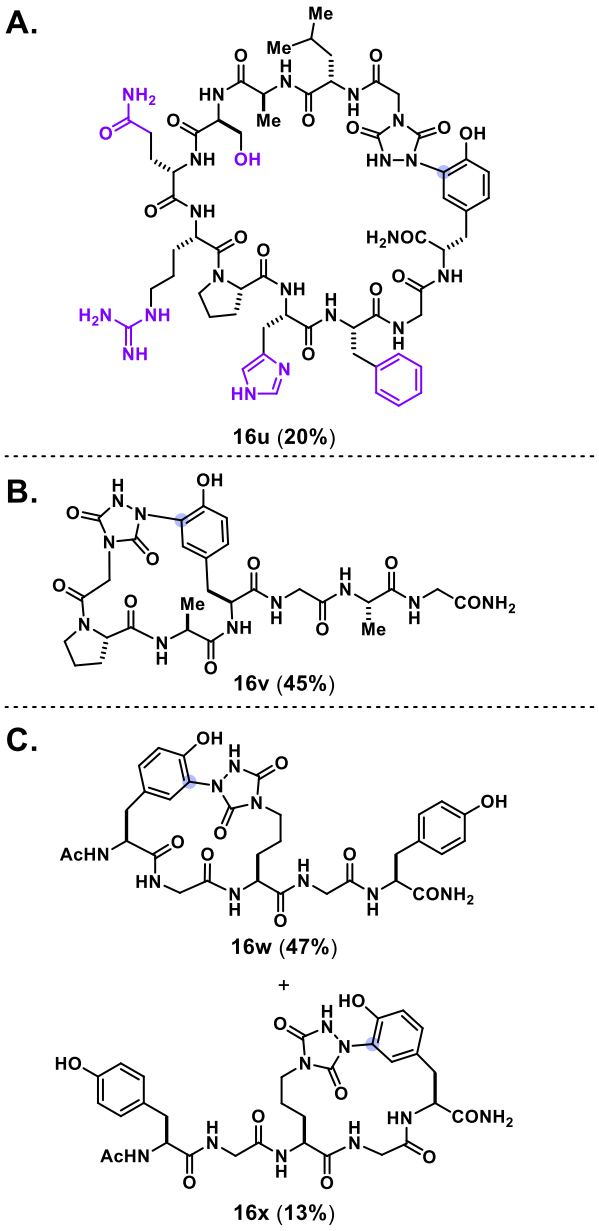

Figure 5. Limitations and selectivity of the presented TAD-based peptide cyclization method. **A.** 11-residue cyclic peptide **16u**, **B.** lariat-type peptide **16v**, **C.** cycles **16w** and **16x**.

cilengitide in separate cell adhesion assays with human umbilical vein endothelial cells (HUVECs) and MCF-7 breast cancer cells, which are known to differentially express αv and α5β1 integrins.[75–77] In both cell lines, no dose dependence differences in cell adherence capability were observed for each of the three peptides (**Figure S134**). Interestingly, in HUVECs, treatment with each peptide resulted in a similar level of reduction in adhesion relative to an untreated control (**Figure 6B**). In contrast, in the phenotypically distinct MCF-7 cells, cilengitide demonstrated a ~10% better ability to reduce cell adhesion relative to **16y** and **16z**. The observed differences in ability to reduce adhesion between peptides in

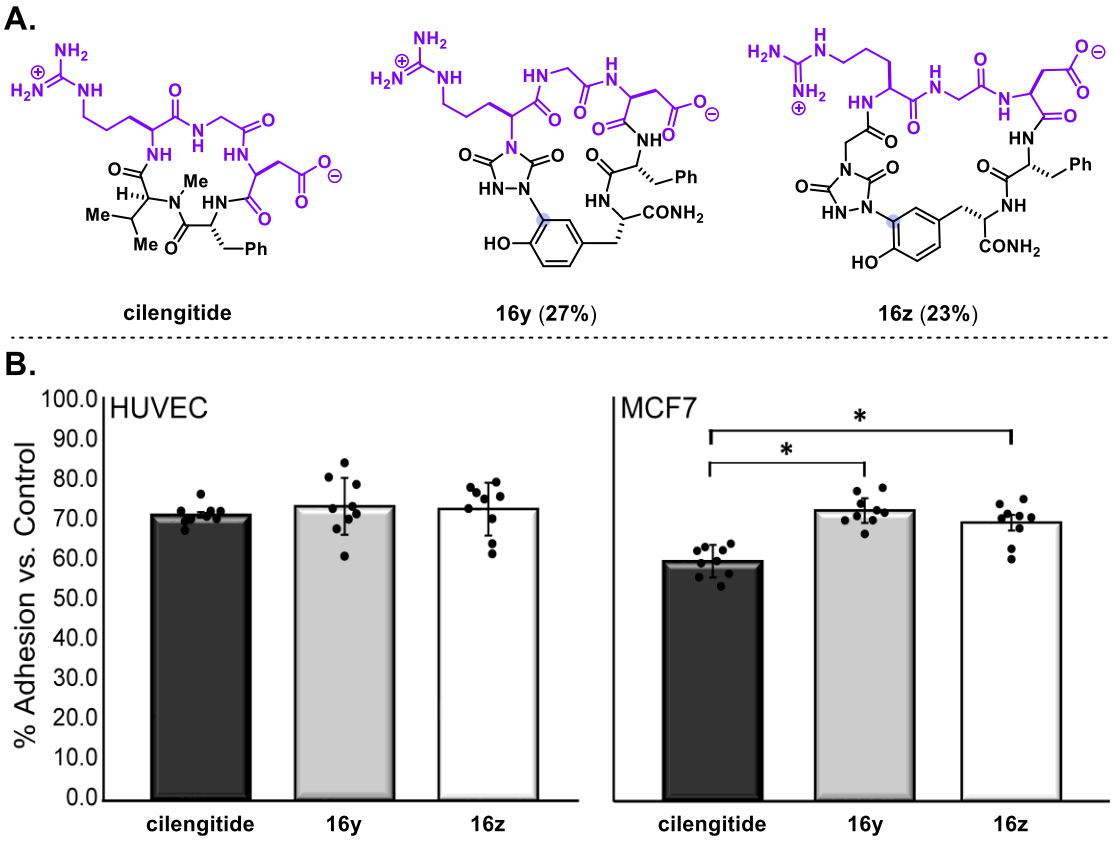

Figure 6. An RGDf epitope imparts cell adhesion inhibition properties to cyclic peptides. **A.** Structures of cilengitide and cyclic peptides **16y** and **16z**. **B.** Results of the cell adhesion assay with HUVECs (left) and MCF7 cells (right). Inhibition of cell adhesion is represented as percentage of adhered cells vs. the untreated control cells. All data are presented as n=3 biological replicates. Error bars reflect the mean ± S.D.; *p<0.05 by Student's t-test.

the two cell lines is likely attributable to the known variances in integrin expression patterns and anchorage dependence between these cell lines.[78–80] While the scope of integrin targeting for cilengitide is well characterized, this has not yet been evaluated for **16y** and **16z**. Nevertheless, these findings demonstrate that the reported cyclization strategy is readily applicable to generate peptides that exhibit biological activity similar to the well-characterized integrin binding molecule cilengitide.

Conclusion

Herein we have reported a novel strategy that leverages *in situ* generated TAD peptides (***int*-16**) to achieve Tyr-selective peptide cyclizations. The requisite urazole-containing peptides (**14**) are selectively oxidized under mild conditions to generate the reactive TAD-peptide intermediates, which are qualitatively characterized by the carmine color characteristic of the TAD chromophore. Upon dilution of the TAD-peptide intermediates using buffered aqueous conditions, cyclization occurs rapidly, and the crude reaction mixture is easily purified to give cyclic peptides (**16**) in good yield. This approach is tolerant of most native residue side chain functionalities and permits access to cyclic peptides that are 3- to 11-residues in size, including lariat-type peptides. Ongoing developments, including the application of electrochemical oxidation protocols should expand residue tolerance to permit the ready incorporation of native Cys, Met, and Trp residues. The application of this method for generating bioactive Tyr-linked cyclic peptides was shown by the formation and evaluation of RGDf epitope-containing Tyr-linked cyclic peptides, **16y** and **16z**, that display adhesion inhibition properties similar to that of cilengitide as determined by separate cell adhesion assays using HUVECs and MCF-7 cells. This result demonstrates the potential application of this chemistry for developing therapeutic peptides and, alongside the procedural simplicity, should render this cyclization strategy as an attractive approach for chemists constructing novel therapeutic peptidomimetic leads.

Associated content

Author information

Corresponding Author
*roberts@chem.utah.edu

Notes
The authors declare no conflicts of interest.

Acknowledgements
We are grateful for the financial support of this research from the University of Utah Department of Chemistry. E.D.K. is thankful for graduate fellowship support from the Professor Gary E. Keck Endowment. M.J.A. and B.J.A. thank the National Science Foundation (NSF) for summer research support through the Research Experiences for Undergraduates program (NSF–REU). M.J.A., B.J.A., and A.S. thank the University of Utah Undergraduate Research Program (UROP) for support of their undergraduate research training. M.J.A. is indebted to the Arnold and Mabel Beckman Foundation for support of his research as a University of Utah Beckman Scholar in the Roberts laboratory. We thank Prof. Ryan E. Looper, Prof. Aaron W. Puri, and Prof. Jon D. Rainier (University of Utah, Department of Chemistry), for insightful discussions and their review of this manuscript. We also thank Dr. Peter Flynn (University of Utah, Department of Chemistry) for assistance with 2D NMR spectroscopy experiments. NMR spectroscopy results included in this report were recorded at the David M. Grant NMR Center, a University of Utah Core Facility. Funds for construction of the Center and the helium recovery system were obtained from the University of Utah and the National Institutes of Health awards 1C06RR017539-01A1 and 3R01GM063540-17W1, respectively. NMR instruments were purchased with support of the University of Utah and the National Institutes of Health award 1S10OD25241-01.

References

(1) Malins, L. R.; Degruyter, J. N.; Robbins, K. J.; Scola, P. M.; Eastgate, M. D.; Ghadiri, M. R.; Baran, P. S. Peptide Macrocyclization Inspired by Non-Ribosomal Imine Natural Products. *J. Am. Chem. Soc.* **2017**, *139* (14), 5233–5241.

(2) Vlieghe, P.; Lisowski, V.; Martinez, J.; Khrestchatisky, M. Synthetic Therapeutic Peptides: Science and Market. *Drug Discov. Today* **2010**, *15* (1–2), 40–56.

(3) Goodwin, D.; Simerska, P.; Toth, I. Peptides As Therapeutics with Enhanced Bioactivity. *Curr. Med. Chem.* **2012**, *19* (26), 4451–4461.

(4) Fosgerau, K.; Hoffmann, T. Peptide Therapeutics: Current Status and Future Directions. *Drug Discov. Today* **2015**, *20* (1), 122–128.

(5) White, C. J.; Yudin, A. K. Contemporary Strategies for Peptide Macrocyclization. *Nat. Chem.* **2011**, *3* (7), 509–524.

(6) Wu, J.; Tang, J.; Chen, H.; He, Y.; Wang, H.; Yao, H. Recent Developments in Peptide Macrocyclization. *Tetrahedron Lett.* **2018**, *59* (4), 325–333.

(7) Driggers, E. M.; Hale, S. P.; Lee, J.; Terrett, N. K. The Exploration of Macrocycles for Drug Discovery - An Underexploited Structural Class. *Nat. Rev. Drug Discov.* **2008**, *7* (7), 608–624.

(8) Vinogradov, A. A.; Yin, Y.; Suga, H. Macrocyclic Peptides as Drug Candidates: Recent Progress and Remaining Challenges. *J. Am. Chem. Soc.* **2019**, *141*, 4167–4181.

(9) Bechtler, C.; Lamers, C. Macrocyclization Strategies for Cyclic Peptides and Peptidomimetics. *RSC Med. Chem.* **2021**, *12* (8), 1325–1351.

(10) Hayes, H. C.; Luk, L. Y. P.; Tsai, Y. H. Approaches for Peptide and Protein Cyclisation. *Org. Biomol. Chem.* **2021**, *19* (18), 3983–4001.

(11) White, A. M.; Craik, D. J. Discovery and Optimization of Peptide Macrocycles. *Expert Opin. Drug Discov.* **2016**, *11* (12), 1151–1163.

(12) Tang, S.; Vincent, G. Natural Products Originated from the Oxidative Coupling of Tyrosine and Tryptophan: Biosynthesis and Bioinspired Synthesis. *Chem. - A Eur. J.* **2021**, *27* (8), 2612–2622.

(13) DeGruyter, J. N.; Malins, L. R.; Baran, P. S. Residue-Specific Peptide Modification: A Chemist's Guide. *Biochemistry* **2017**, *56* (30), 3863–3873.

(14) Cherfan, D.; Verter, E. E.; Melki, S.; Gisel, T. E.; Doyle, F. J.; Scarcelli, G.; Yun, S. H.; Redmond, R. W.; Kochevar, I. E. Collagen Cross-Linking Using Rose Bengal and Green Light to Increase Corneal Stiffness. *Investig. Ophthalmol. Vis. Sci.* **2013**, *54* (5), 3426–3433.

(15) Malencik, D. A.; Anderson, S. R. Dityrosine as a Product of Oxidative Stress and Fluorescent Probe. *Amino Acids* **2003**, *25* (3–4), 233–247.

(16) Keyes, E. D.; Kauser, K.; Warner, K. S.; Roberts, A. G. Photosensitized Oxidative Dimerization at Tyrosine by a Water-Soluble 4-Amino-1,8-Naphthalimide. *ChemBioChem* **2021**, *22* (17), 2703–2710.

(17) Rhodes, C. A.; Pei, D. Bicyclic Peptides as Next-Generation Therapeutics. *Chem. A Eur. J.* **2017**, *23*, 12690–12703.

(18) Kase, H.; Kaneko, M.; Yamada, K. K-13, A Novel Inhibitor of Angiotensin I Converting Enzyme Produced by Micromonospora Halophytica Subsp. Exilisia I. Fermentation, Isolation, and Biological Properties. *J. Antibiot. (Tokyo).* **1987**, *40*, 450–454.

(19) Janetka, J. W.; Rich, D. H. Total Synthesis of the Cyclic Biphenyl Ether Peptides K-13 and OF494-III via S(N)Ar Macrocyclizations of Peptidyl Ruthenium π-Arene Complexes. *J. Am. Chem. Soc.* **1997**, *119* (28), 6488–6495.

(20) Zhao, Y.; Marschall, E.; Treisman, M.; McKay, A.;

Padva, L.; Crüsemann, M.; Nelson, D. R.; Steer, D. L.; Schittenhelm, R. B.; Tailhades, J.; Cryle, M. J. Cytochrome P450 Blt Enables Versatile Peptide Cyclisation to Generate Histidine- and Tyrosine-Containing Crosslinked Tripeptide Building Blocks. *Angew. Chemie Int. Ed.* **2022**, *61*, 1–7.

(21) Boger, D. L.; Miyazaki, S.; Heon Kim, S.; Wu, J. H.; Castle, S. L.; Loiseleur, O.; Jin, Q. Total Synthesis of the Vancomycin Aglycon. *J. Am. Chem. Soc.* **1999**, *121* (3), 10004–10011.

(22) Holtzel, A.; Schmid, D. G.; Nicholson, G. J.; Stevanovic, S.; Schimana, J.; Gebhardt, K.; Fiedler, H.-P.; Jung, G. Arylomycins A and B, New Biaryl-Bridged Lipopeptide Antibiotics Produced by Streptomyces Sp. Tu 6075. *J. Antibiot. (Tokyo).* **2002**, *55* (6), 571–577.

(23) Roberts, T. C.; Smith, P. A.; Cirz, R. T.; Romesberg, F. E. Structural and Initial Biological Analysis of Synthetic Arylomycin A2. *J. Am. Chem. Soc.* **2007**, *129*, 15830–15838.

(24) Reguera, L.; Rivera, D. G. Multicomponent Reaction Toolbox for Peptide Macrocyclization and Stapling. *Chem. Rev.* **2019**, *119*, 9836–9860.

(25) Gisemba, S. A.; Aldrich, J. V. Optimized Ring Closing Metathesis Reaction Conditions To Suppress Desallyl Side Products in the Solid-Phase Synthesis of Cyclic Peptides Involving Tyrosine(O-Allyl). *J. Org. Chem* **2020**, *85*, 1407–1415.

(26) Smith, P. A.; Koehler, M. F. T.; Girgis, H. S.; Yan, D.; Chen, Y.; Chen, Y.; Crawford, J. J.; Durk, M. R.; Higuchi, R. I.; Kang, J.; Murray, J.; Paraselli, P.; Park, S.; Phung, W.; Quinn, J. G.; Roberts, T. C.; Rougé, L.; Schwarz, J. B.; Skippington, E.; Wai, J.; Xu, M.; Yu, Z.; Zhang, H.; Tan, M.-W.; Heise, C. E. Optimized Arylomycins Are a New Class of Gram-Negative Antibiotics. *Nature* **2018**, *561*, 189–194.

(27) Sengupta, S.; Mehta, G. Macrocyclization via C-H Functionalization: A New Paradigm in Macrocycle Synthesis. *Org. Biomol. Chem.* **2020**, *18*, 1851–1876.

(28) Rivera, D. G.; Ojeda-Carralero, G. M.; Reguera, L.; Van Der Eycken, E. V. Peptide Macrocyclization by Transition Metal Catalysis. *Chem. Soc. Rev.* **2020**, *49* (7), 2039–2059.

(29) Peters, D. S.; Romesberg, F. E.; Baran, P. S. Scalable Access to Arylomycins via C-H Functionalization Logic. *J. Am. Chem. Soc.* **2018**, *140* (6), 2072–2075.

(30) Tilley, S. D.; Francis, M. B. Tyrosine-Selective Protein Alkylation Using π-Allylpalladium Complexes. *J. Am. Chem. Soc.* **2006**, *128* (4), 1080–1081.

(31) Sato, S.; Nakamura, K.; Nakamura, H. Tyrosine-Specific Chemical Modification with in Situ Hemin-Activated Luminol Derivatives. *ACS Chem. Biol.* **2015**, *10* (11), 2633–2640.

(32) Rose, T. E.; Lawson, K. V.; Harran, P. G. Large Ring-Forming Alkylations Provide Facile Access to Composite Macrocycles. *Chem. Sci.* **2015**, *6* (4), 2219–2223.

(33) Sato, S.; Nakane, K.; Nakamura, H. A Laccase-Catalysed Tyrosine Click Reaction. *Org. Biomol. Chem.* **2020**, *18* (19), 3664–3668.

(34) Depienne, S.; Alvarez-Dorta, D.; Croyal, M.; Temgoua, R. C. T.; Charlier, C.; Deniaud, D.; Mével, M.; Boujtita, M.; Gouin, S. G. Luminol Anchors Improve the Electrochemical-Tyrosine-Click Labelling of Proteins. *Chem. Sci.* **2021**, *12* (46), 15374–15381.

(35) Sato, S.; Hatano, K.; Tsushima, M.; Nakamura, H. 1-Methyl-4-Aryl-Urazole (MAUra) Labels Tyrosine in Proximity to Ruthenium Photocatalysts. *Chem. Commun.* **2018**, *54* (46), 5871–5874.

(36) Huang, F.; Nie, Y.; Ye, F.; Zhang, M.; Xia, J. Site Selective Azo Coupling for Peptide Cyclization and Affinity Labeling of an SH3 Protein. *Bioconjug. Chem.* **2015**, *26* (8), 1613–1622.

(37) Joshi, N. S.; Whitaker, L. R.; Francis, M. B. A Three-Component Mannich-Type Reaction for Selective Tyrosine Bioconjugation. *J. Am. Chem. Soc.* **2004**, *126* (49), 15942–15943.

(38) Seim, K. L.; Obermeyer, A. C.; Francis, M. B. Oxidative Modification of Native Protein Residues Using Cerium(IV) Ammonium Nitrate. *J. Am. Chem. Soc.* **2011**, *133* (42), 16970–16976.

(39) Zhao, H.; Negash, L.; Wei, Q.; LaCour, T. G.; Estill, S. J.; Capota, E.; Pieper, A. A.; Harran, P. G. Acid Promoted Cinnamyl Ion Mobility within Peptide Derived Macrocycles. *J. Am. Chem. Soc.* **2008**, *130* (42), 13864–13866.

(40) Lawson, K. È.; Rose, T. E.; Harran, P. G. Template-Constrained Macrocyclic Peptides Prepared from Natièe, Unprotected Precursors. *Proc. Natl. Acad. Sci. U. S. A.* **2013**, *110* (40), 3753–3760.

(41) Molinaro, C.; Kawasaki, Y.; Wanyoike, G.; Nishioka, T.; Yamamoto, T.; Snedecor, B.; Robinson, S. J.; Gosselin, F. Engineered Cytochrome P450-Catalyzed Oxidative Biaryl Coupling Reaction Provides a Scalable Entry into Arylomycin Antibiotics. *J. Am. Chem. Soc.* **2022**, *144* (32), 14838–14845.

(42) Wang, T.; Danishefsky, S. J. Solid-Phase Peptide Synthesis and Solid-Phase Fragment Coupling Mediated by Isonitriles. *Proc. Natl. Acad. Sci. U. S. A.* **2013**, *110* (29), 11708–11713.

(43) Caruso, A.; Martinie, R. J.; Bushin, L. B.; Seyedsayamdost, M. R. Macrocyclization via an Arginine-Tyrosine Crosslink Broadens the Reaction Scope of Radical S-Adenosylmethionine Enzymes. *J. Am. Chem. Soc.* **2019**, *141* (42), 16610–16614.

(44) Laws, D.; Plouch, E. V.; Blakey, S. B. Synthesis of Ribosomally Synthesized and Post-Translationally Modified Peptides Containing C-C Cross-Links. *J. Nat. Prod.* **2022**, *85*, 2519–2539.

(45) Barbas, C. F.; Ban, H.; Gavrilyuk, J. Tyrosine Bioconjugation through Aqueous Ene-Type

Reactions: A Click-like Reaction for Tyrosine. *J. Am. Chem. Soc.* **2010**, *132* (5), 1523–1525.
(46) Moinpour, M.; Barker, N. K.; Guzman, L. E.; Jewett, J. C.; Langlais, P. R.; Schwartz, J. C. Discriminating Changes in Protein Structure Using Tyrosine Conjugation. *Protein Sci.* **2020**, *29* (8), 1784–1793.
(47) Ban, H.; Nagano, M.; Gavrilyuk, J.; Hakamata, W.; Inokuma, T.; Barbas, C. F. Facile and Stabile Linkages through Tyrosine: Bioconjugation Strategies with the Tyrosine-Click Reaction. *Bioconjug. Chem.* **2013**, *24* (4), 520–532.
(48) Sato, S.; Matsumura, M.; Kadonosono, T.; Abe, S.; Ueno, T.; Ueda, H.; Nakamura, H. Site-Selective Protein Chemical Modification of Exposed Tyrosine Residues Using Tyrosine Click Reaction. *Bioconjug. Chem.* **2020**, *31* (5), 1417–1424.
(49) Al-Momani, E.; Israel, I.; Buck, A. K.; Samnick, S. Improved Synthesis of [18F]FS-PTAD as a New Tyrosine-Specific Prosthetic Group for Radiofluorination of Biomolecules. *Appl. Radiat. Isot.* **2015**, *104*, 136–142.
(50) Jessica, F.; Corentin, W.; Sylvestre, D.; Christian, L.; André, L. Synthesis of [18F]4-(4-Fluorophenyl)-1,2,4-Triazole-3,5-Dione: An Agent for Specific Radiolabelling of Tyrosine. *RSC Adv.* **2013**, *3* (47), 24936–24940.
(51) Decoene, K. W.; Unal, K.; Staes, A.; Zwaenepoel, O.; Gettemans, J.; Gevaert, K.; Winne, J. M.; Madder, A. Triazolinedione Protein Modification: From an Overlooked off-Target Effect to a Tryptophan-Based Bioconjugation Strategy. *Chem. Sci.* **2022**, *13* (18), 5390–5397.
(52) Schwartz, B. D.; Smyth, A. P.; Nashar, P. E.; Gardiner, M. G.; Malins, L. R. Investigating Bicyclobutane-Triazolinedione Cycloadditions as a Tool for Peptide Modification. *Org. Lett.* **2022**, *24*, 1268–1273.
(53) Chattopadhyay, S.; Du Prez, F. E.; Kunde, T.; ten Brummelhuis, N.; Börner, H. G.; Wilke, P. Easy Access to Triazolinedione-Endcapped Peptides for Chemical Ligation. *Chem. Commun.* **2016**, *53* (3), 593–596.
(54) Oves, D.; Ferrero, M.; Fernández, S.; Gotor, V. Efficient Synthesis of Novel 4-Substituted Urazoles. *Synth. Commun.* **2002**, *32*, 1741–1749.
(55) Alvarez-Dorta, D.; Thobie-Gautier, C.; Croyal, M.; Bouzelha, M.; Mével, M.; Deniaud, D.; Boujtita, M.; Gouin, S. G. Electrochemically Promoted Tyrosine-Click-Chemistry for Protein Labeling. *J. Am. Chem. Soc.* **2018**, *140* (49), 17120–17126.
(56) Fernández-Herrera, M. A.; Sandoval-Ramírez, J.; Montiel-Smith, S.; Meza-Reyes, S. A Convenient Methodology for the in Situ Oxidation of 4-Substituted Urazoles. Setting UP a One-Pot Procedure for the Efficient Protection of Dienes. *Heterocycles* **2013**, *87* (3), 571–582.
(57) Agouridas, V.; El Mahdi, O.; Diemer, V.; Cargoët, M.; Monbaliu, J. C. M.; Melnyk, O. Native Chemical Ligation and Extended Methods: Mechanisms, Catalysis, Scope, and Limitations. *Chem. Rev.* **2019**, *119* (12), 7328–7443.
(58) De Bruycker, K.; Billiet, S.; Houck, H. A.; Chattopadhyay, S.; Winne, J. M.; Du Prez, F. E. Triazolinediones as Highly Enabling Synthetic Tools. *Chem. Rev.* **2016**, *116* (6), 3919–3974.
(59) Schuster, D. I.; Wang, L.; van der Veen, J. M. Photodecarbonylation of Cis- and Trans-2,7-Dimethyl-3,5-Cycloheptadienones: Applicability of Orbital Symmetry Theory to Photochemical Cheletropic Fragmentations. *J. Am. Chem. Soc.* **1985**, *107*, 7045–7053.
(60) Koley, D.; Colón, O. C.; Savlnov, S. N. Chemoselective Nitration of Phenols with Tert-Butyl Nitrite in Solution and on Solid Support. *Org. Lett.* **2009**, *11* (18), 4172–4175.
(61) Hanay, S. B.; Ritzen, B.; Brougham, D.; Dias, A. A.; Heise, A. Exploring Tyrosine-Triazolinedione (TAD) Reactions for the Selective Conjugation and Cross-Linking of N-Carboxyanhydride (NCA) Derived Synthetic Copolypeptides. *Macromol. Biosci.* **2017**, *17* (7), 1–7.
(62) Zolfigol, M. A.; Madrakian, E.; Ghaemi, E.; Mallakpour, S. Trichloroisocyanuric Acid as a Novel Oxidizing Agent for the Oxidation of Urazoles Under Both Heterogeneous and Solvent Free Conditions. *Synlett* **2002**, *10*, 1633–1636.
(63) Gołębiewski, W. M.; Gucma, M. Applications of N-Chlorosuccinimide in Organic Synthesis. *Synthesis (Stuttg).* **2007**, No. 23, 3599–3619.
(64) Baran, P. S.; Guerrero, C. A.; Corey, E. J. The First Method for Protection-Deprotection of the Indole 2,3-π Bond. *Org. Lett.* **2003**, *5* (11), 1999–2001.
(65) Hanay, S. B.; Brougham, D. F.; Dias, A. A.; Heise, A. Investigation of the Triazolinedione (TAD) Reaction with Tryptophan as a Direct Route to Copolypeptide Conjugation and Cross-Linking. *Polym. Chem.* **2017**, *8* (43), 6594–6597.
(66) Martí-Centelles, V.; Pandey, M. D.; Burguete, M. I.; Luis, S. V. Macrocyclization Reactions: The Importance of Conformational, Configurational, and Template-Induced Preorganization. *Chem. Rev.* **2015**, *115*, 8736–8834.
(67) Kelly, C. N.; Townsend, C. E.; Jain, A. N.; Naylor, M. R.; Pye, C. R.; Schwochert, J.; Lokey, R. S. Geometrically Diverse Lariat Peptide Scaffolds Reveal an Untapped Chemical Space of High Membrane Permeability. *J. Am. Chem. Soc.* **2021**, *143* (2), 705–714.
(68) Mas-Moruno, C.; Rechenmacher, F.; Kessler, H. Cilengitide: The First Anti-Angiogenic Small Molecule Drug Candidate. Design, Synthesis and Clinical Evaluation. *Anticancer. Agents Med. Chem.* **2010**, *10*, 753–768.
(69) Dechantsreiter, M. A.; Planker, E.; Matha, B.; Lohof, E.; Jonczyk, A.; Goodman, S. L.; Kessler, H.

N-Methylated Cyclic RGD Peptides as Highly Active and Selective AVβ3 Integrin Antagonists. *J. Med. Chem.* **1999**, *42*, 3033–3040.

(70) Maurer, G. D.; Tritschler, I.; Adams, B.; Tabatabai, G.; Wick, W.; Stupp, R.; Weller, M. Cilengitide Modulates Attachment and Viability of Human Glioma Cells, but Not Sensitivity to Irradiation or Temozolomide in Vitro. *Neuro. Oncol.* **2009**, *11* (6), 747–756.

(71) Avraamides, C. J.; Garmy-Susini, B.; Varner, J. A. Integrins in Angiogenesis and Lymphangiogenesis. *Nat. Rev. Cancer* **2008**, *8* (8), 604–617.

(72) Rechenmacher, F.; Neubauer, S.; Polleux, J.; Mas-Moruno, C.; De Simone, M.; Cavalcanti-Adam, E. A.; Spatz, J. P.; Fässler, R.; Kessler, H. Functionalizing Avβ3- or A5β1-Selective Integrin Antagonists for Surface Coating: A Method to Discriminate Integrin Subtypes in Vitro. *Angew. Chemie - Int. Ed.* **2013**, *52* (5), 1572–1575.

(73) Reardon, D. A.; Neyns, B.; Weller, M.; Tonn, J. C.; Nabors, L. B.; Stupp, R. Cilengitide: An RGD Pentapeptide Avβ3 and Avβ5 Integrin Inhibitor in Development for Glioblastoma and Other Malignancies. *Futur. Oncol.* **2011**, *7*, 339–354.

(74) Conibear, A. C.; Chaousis, S.; Durek, T.; Johan Rosengren, K.; Craik, D. J.; Schroeder, C. I. Approaches to the Stabilization of Bioactive Epitopes by Grafting and Peptide Cyclization. *Biopolymers* **2016**, *106* (1), 89–100.

(75) Mosayyebi, B.; Mohammadi, L.; Kalantary-Charvadeh, A.; Rahmati, M. Amygdalin Decreases Adhesion and Migration of MDA-MB-231 and MCF-7 Breast Cancer Cell Lines. *Curr. Mol. Pharmacol.* **2020**, *14* (4), 667–675.

(76) Hegemann, J. D.; De Simone, M.; Zimmermann, M.; Knappe, T. A.; Xie, X.; Di Leva, F. S.; Marinelli, L.; Novellino, E.; Zahler, S.; Kessler, H.; Marahiel, M. A. Rational Improvement of the Affinity and Selectivity of Integrin Binding of Grafted Lasso Peptides. *J. Med. Chem.* **2014**, *57* (13), 5829–5834.

(77) Hou, J.; Yan, D.; Liu, Y.; Huang, P.; Cui, H. The Roles of Integrin A5B1 in Human Cancer. *Onco. Targets. Ther.* **2020**, *13*, 13329–13344.

(78) Yao, L.; Chen, H.; Chen, Z. Dual Targeting of Integrin Avβ3 and VEGF Receptor Improves PET Imaging of Breast Cancer. *Res. Sq.* **2021**, preprint article.

(79) Forster-Horváth, C.; Mészáros, L.; Rásó, E.; Döme, B.; Ladányi, A.; Morini, M.; Albini, A.; Tímár, J. Expression of CD44v3 Protein in Human Endothelial Cells in Vitro and in Tumoral Microvessels in Vivo. *Microvasc. Res.* **2004**, *68* (2), 110–118.

(80) Hida, K.; Hida, Y.; Shindoh, M. Understanding Tumor Endothelial Cell Abnormalities to Develop Ideal Anti-Angiogenic Therapies. *Cancer Sci.* **2008**, *99*, 459–466.